

13.1 Ground-based damage survey and radar analysis of the El Reno, Oklahoma Tornado

Timothy P. Marshall¹, D. Burgess², G. Garfield², R. Smith³, D. Speheger³, J. Snyder⁴, H. Bluestein⁴

¹Haag Engineering Company, Irving Texas

²University of Oklahoma/CIMMS

³NOAA/NWS

⁴University of Oklahoma

1. INTRODUCTION

On 31 May 2013, an intense, multiple-vortex tornado meandered through sparsely populated areas near El Reno, Oklahoma (Fig. 1). This exceptionally wide tornado had a complex path, changing rapidly in both speed and direction (Fig. 2). The tornado killed eight people, all in vehicles, including three severe storm researchers (NWS, 2013). Storm survey teams traveled to the area the next day and rated 257 DIs (damage indicators) using the EF (Enhanced Fujita) scale developed by the Wind Science and Engineering Center (WSEC, 2006). Survey teams also documented damage to 344 non-standard DIs which included 112 oil tank batteries. The maximum damage rating was determined to be EF3. Total path length was 26.2 km.

In addition, the tornado was well sampled at close range by the University of Oklahoma's Rapid-Scan, X-band, Polarimetric, mobile Doppler radar (RaXPol). The radar obtained high temporal and spatial resolution velocity data indicating instantaneous winds in excess of 130 m s^{-1} close to the ground surface. Intense winds were present in small subvortices within the larger tornadic circulation. Analysis of the high resolution radar data combined with results of the ground damage survey indicated that none of the intense subvortices struck any structures. So, despite the high radar-derived wind velocities, surveyors could not find damage that would support a rating higher than EF3.

In this paper, we present the results of our ground-based damage survey and compare EF ratings with the maximum radial velocities obtained by the RaXPol radar. In general, we found that RaXPol velocity measurements were 10 to 30 percent higher than EF scale values.

We refer to Atkins et al. (2014) for an aerial study of the El Reno damage track. Also, Wakimoto et al. (2014) performed photogrammetric analyses of the

El Reno tornado and compared them to RaXPol velocity data. Wurman et al. (2014) performed a detailed analysis of radar data from Doppler on Wheels (DOWs) radars near the El Reno tornado and also found high velocities in subvortices.



Figure 1. Wedge-shaped tornado approaching from the southwest taken from 0.8 km east of Radio and Jensen roads at 2326 UTC. The tornado crossed the image location approximately two minutes later. Image by Tim Marshall.

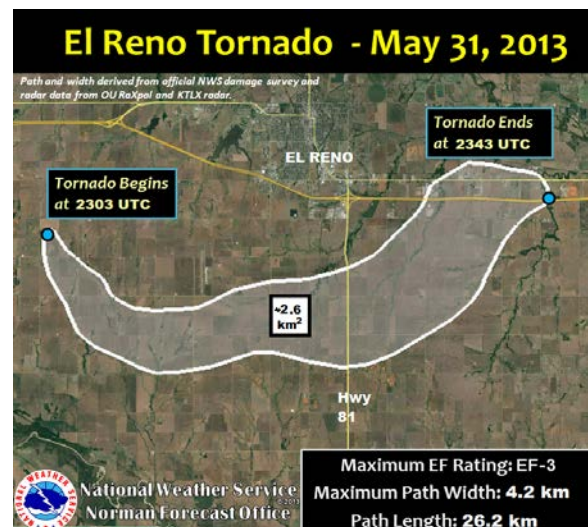


Figure 2. Track of the El Reno OK tornado with approximate boundaries (white outline). Times in UTC are shown along with major roads and the location of El Reno. Map courtesy of NOAA/NWS.

Corresponding author address: Timothy P. Marshall, 4949 West Royal Lane, Irving, Texas 75063. Email: timpmarshall@cs.com.

2. DAMAGE SURVEY LOGISTICS

The morning after the El Reno tornado, Don Burgess, Gabe Garfield, and Tim Marshall departed Norman to survey the damage. The primary goals of the damage survey were to: 1) document all substantial damage, 2) document the most extreme damage, 3) estimate the path width, and 4) estimate the path length. In order to record our observations, the teams used voice memos, note pads, and the Damage Assessment Toolkit (DAT). The toolkit can be used to plot latitudes and longitudes of DIs on a topographical map and has a phone application. The survey crew obtained “representative” images of the damage using cell phone cameras. Information recorded during the survey included the type of DI, the DoD, the EF rating, as well as additional notes. Generally, the DAT worked well, although heavy use of the DAT quickly drained cell phone batteries. Therefore, it is important that survey teams using the DAT come equipped with car phone chargers.

Initially, the team investigated damage west of Highway 81 and discovered up to EF3 damage. Later that afternoon, the team drove east of Highway 81 to document damage where, according to WSR-88D data, the tornado likely reached maximum intensity. However, there were few structures within this region of most intense winds, and damage only up to EF3 was found.

The next day, a second damage survey team, comprised of Marc Austin, Don Burgess, Gabe Garfield, and Jeff Snyder continued to analyze tornado damage. The team split into two groups. One group (Burgess and Snyder) continued to look for extreme damage, while the other group (Austin and Garfield) sought to document the path width and length.

Burgess and Snyder investigated the area near Reuter and Radio roads, where the most extreme winds were recorded by RaXPOL radar. There were no buildings in this area, but the team found scoured road gravel and curved swaths of flattened wheat. Swaths of flattened wheat were as narrow as 1 m wide and up to 30 m long. These smaller swaths left distinct, independent paths. However, in one instance, it appeared a pair of smaller subvortices had rotated around each other, creating a double-helix pattern in a wheat field. Some swaths also appeared to have been caused by debris trajectories.

Meanwhile, Austin and Garfield searched for the beginning of the path west of Highway 81. They discovered minor tree damage associated with the initial circulation of the tornado near the intersection of Jensen and Red Rock roads. Farther south and east, team members discovered more severe damage near the intersection of Jensen and Heaston roads.

There, strong winds had peeled away the roof of a metal outbuilding.

Once the survey team determined where the tornado had touched down initially, the focus shifted to determining the width of the tornado. The team made north-south transects using a car odometer and the DAT to mark the width of the tornado path. The team encountered several difficulties in accurately determining the tornado width: a) the direction of the tornado changed several times, so north-south transects were often oblique to the tornado track and, thus, widths of the damage path were often overestimated; b) the rural nature of the path made it difficult to determine the edge of the path; and c) the presence of rear-flank downdraft (RFD) damage made it difficult to distinguish that damage from the tornado damage. After completing transects, team members located the end of the path near Interstate 40 and Banner Road.

Teams rated and plotted a total of 257 DIs on a DAT map and identified an additional 344 non-standard DIs which included 112 oil tank batteries (Fig. 3).

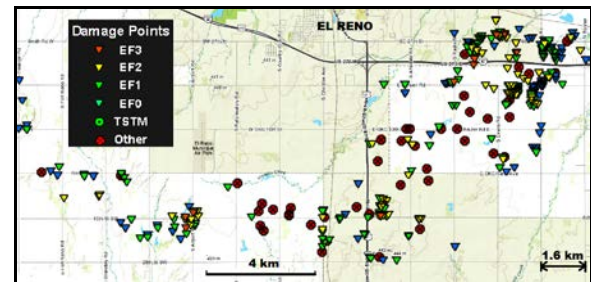


Figure 3. DAT plot of DIs and non-standard DIs for the El Reno tornado. EF-scale intensity is shown by the colored triangles. Non-standard DIs (including oil tank sites) are indicated by red dots.

Tornado damage occurred within 39 square mile blocks (Fig. 4). The number of DIs was not uniform along the tornado path but concentrated near the end of the tornado path, near Interstate 40. There were 25 square mile blocks with fewer than 10 DIs each. By comparison, the greatest number of DIs per square mile was 69 due to a concentration of manufactured homes just south of Interstate 40.

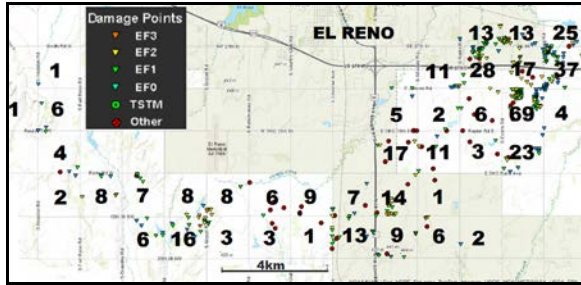


Figure 4. DAT plot showing the numbers of DIs per square mile in the El Reno tornado. The greatest concentration of DIs occurred near the end of the tornado path, near Interstate 40.

Though survey goals (1), (2), and (4) were met, the maximum path width dimension remained uncertain. Thus, team members sought high-resolution data collected by the RaXPoI radar during the El Reno tornado (Fig. 5). Analysis of velocity data indicated a sharp gradient around the 30 m s^{-1} isodop, between ambient winds and much higher winds. Also, our ground based survey confirmed damage in areas where V_{max} was 30 m s^{-1} or greater. Thus, the 30 m s^{-1} isodop was selected as the boundary of the tornado. Using the 30 m s^{-1} isodop, the team estimated the width of the tornado was at least 4.2 km, a new record for tornado width. Previous to the El Reno tornado, the widest tornado in recorded United States history was the Hallam, Nebraska F4 tornado of 22 May 2004 (Adams, 2005).

RaXPoI data were utilized to determine the width of the tornado along its entire path (with the exception of the period from 23:17:48 to 23:24:09 UTC while the radar truck relocated). The procedure for determining the width of the tornado path was fairly straight forward. First, center points of the tornado were determined from the RaXPoI data. Second, edges of the tornado were determined using the 30 m s^{-1} isodop. Third, (since we were working with radial components of the tornado winds) we rotated the radar-estimated tornado widths about the radar-estimated centers in order to align orthogonally with the tornado motion vectors (while preserving the width). This final step determined the edges of the tornado.

The RaXPoI radar was located optimally to acquire wind velocities near the ground. The radar truck was parked on a highway overpass at Interstate 40 and Banner Road and scanned the tornado while it was in its most intense phase. At that time, the radar beam was centered at zero degree elevation causing a portion of the beam to intersect the ground near the tornado about 3 km to the southwest.



Figure 5. The University of Oklahoma's RaXPoI radar which scanned the El Reno tornado.

3. DAMAGE TRACK OVERVIEW

The tornado developed around 2303 UTC in a sparsely populated area about 10 km west of El Reno (Fig. 6). Initially, the tornado traveled southeast causing occasional EF0 and EF1 damage to rural homes and outbuildings. On average, there were about 4 DIs per square mile. The first EF2 damage occurred to a home which lost its roof on South Brandley Road. Storm chasers had observed a multi-vortex tornado at this time which continued to widen.

Around 2309 UTC, the tornado turned east as it crossed Chiles Road and paralleled, but did not cross, SW 29th Street to the south. At this time, the tornado damage track was approximately 2.6 km wide. The tornado struck several oil tank batteries causing little to no damage. Damage to rural homes remained in the EF0 to EF1 range. Then, the core of the tornado passed through a subdivision consisting of about a dozen homes and inflicted up to EF3 damage. Roofs were removed and perimeter walls were toppled on three homes, leaving only interior walls standing.

As the tornado passed south of the El Reno Municipal Airport, it again traversed sparsely populated areas with only a small number of DIs (Figure 7). However, the tornado struck more than a dozen oil tank batteries. Oil tank batteries consisted of one or more steel tanks, a gas separator tank, and occasional heater treater tanks. These items were not anchored to the ground. Gas separator tanks were oriented either vertically or horizontally and sat on concrete pads. Heater treaters were tall vertical tanks that also sat on concrete pads. Along 15th Street, a steel tank overturned to the north while a separator tank fell to the northwest on an adjacent facility.

As the tornado approached Highway 81, about 6 km south of El Reno, it reached its maximum width of 4.2 km, at about 2319 UTC. Team members observed the most severe damage to oil tank batteries in this area. Six sites had tanks knocked over or missing. Some of these tanks rolled as far as 4 km.

Along Highway 81, there was a blue painted steel water tank that escaped damage in the southern edge of the tornado. However, an adjacent residence sustained EF1 damage.

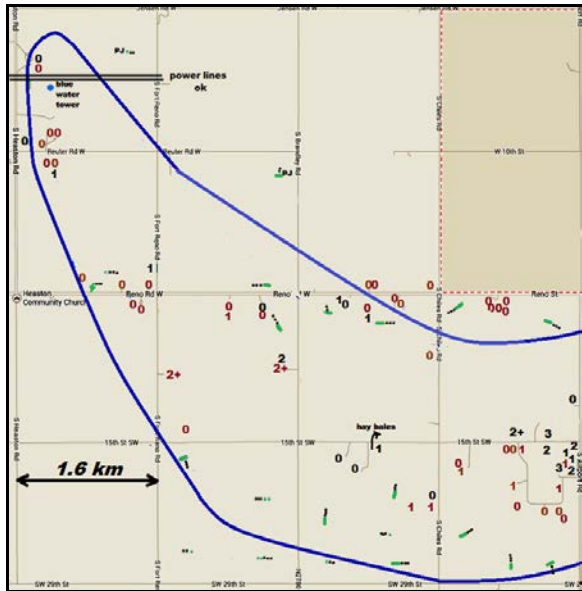


Figure 6. The beginning of the tornado damage path showing EF ratings. The blue outline is the approximate boundary of the tornado damage track determined by analysis of RaXPol velocity data. Oil tank batteries are black dots. Gas separators and heater treaters are green dots. The initials “PJ” indicate pump jacks. Arrows indicate the directions various items were moved.

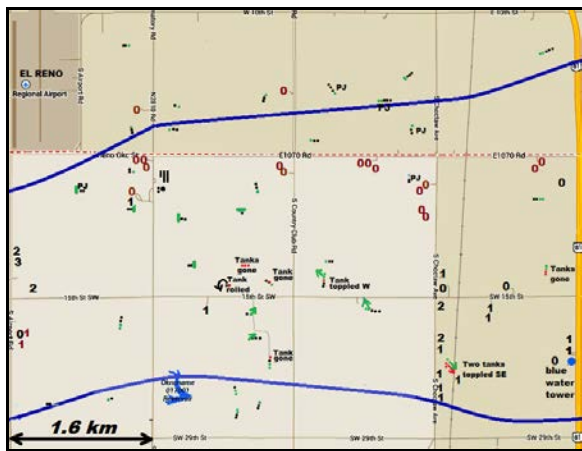


Figure 7. The tornado damage path between the El Reno Regional Airport and Highway 81 showing EF ratings. The remaining caption is the same as Figure 6.

After crossing Highway 81, the tornado struck a subdivision of ten homes along SW 15th Street causing up to EF3 damage (Fig. 8). Here, several people sought refuge in underground shelters. It was at this time that the tornado began to turn northeast and intensify. Oil tank batteries were damaged in a swath that extended 4 km wide and most of the damage consisted of toppled gas separators and heater treaters. Four gas separator tanks fell in a converging pattern near Alfadale Road at four different sites. A portion of the wheat crop was flattened near Reuter Road but was not scoured. Also, some loose gravel was scoured in two locations along Reuter Road. Three storm researchers were killed when their vehicle was blown off Reuter Road around 2323 UTC. Numerous trees were uprooted in the creek bed on both sides of Reuter Road, yielding EF1 ratings.

As the tornado continued northeast, it struck a subdivision south of Jensen Road containing about 60 manufactured homes (Fig 9). A few homes were completely destroyed yielding EF2 ratings. Along Interstate 40, the tornado downed 15 pairs of wood power poles over a distance of 3km. Just north of Interstate 40, three metal buildings were destroyed at the Oklahoma West Cattle Market. The buildings failed where steel columns were bolted to the concrete slabs.

The tornado then struck the Canadian Valley Technology Center (El Reno Campus) along historic Route 66. The campus consisted of three, one-story, steel-reinforced concrete structures and a variety of smaller buildings. There were various degrees of damage to the buildings, but none of the buildings sustained more than EF3 damage. Interestingly, a turbine blade mounted on a pedestal for display purposes was blown onto one of the school buildings. Also, some of the concrete stops in the parking lot were shifted by low-level tornadic winds.

The translational speed of the tornado slowed after it crossed Interstate 40 and made an abrupt turn or loop to the east before dissipating near Banner Road around 2343 UTC. The final point of damage was at a Shell gas station which sustained minor damage to its marquee sign and canopy. Overall, damage caused by this tornado was moderate being less severe than observed at Plainfield in 1990, Jarrell in 1997, and Bridge Creek in 1999. In each of those tornadoes, substantial ground scouring occurred.

A color map of the El Reno tornado was drawn (Fig. 10). EF ratings were smoothed, contoured, and colored. Overall, team members found three distinct spots of EF3 damage.

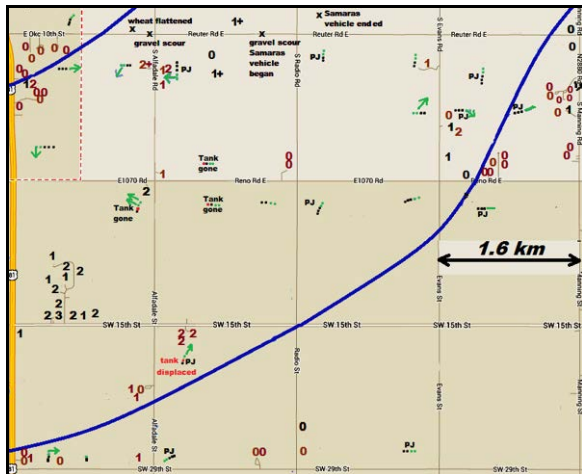


Figure 8. The tornado damage path east of Highway 81 and south of Reuter Road showing EF ratings. The remaining caption is the same as Figure 6.

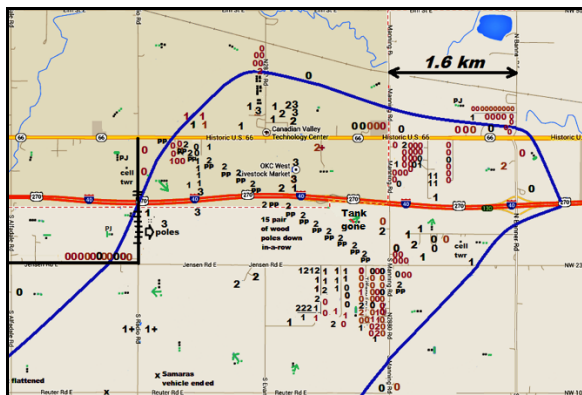


Figure 9. Terminus of the tornado damage path along Interstate 40 east of El Reno showing EF ratings. The remaining caption is the same as Figure 6.

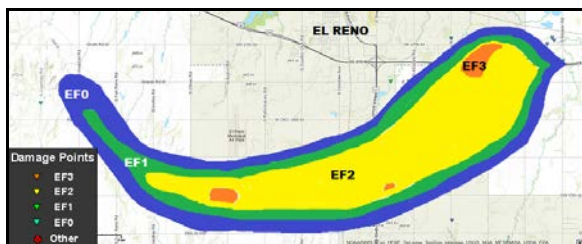


Figure 10. Contoured and colored map of EF ratings for the El Reno tornado. There were three distinct spots of EF3 damage.

4. SPECIFIC DIs

In this section, specific DIs will be discussed. The most common DIs rated were outbuildings, wood-framed houses, and manufactured homes. The following list of DI's appears in the same order as in the EF scale document.

4.1 Outbuildings – DI 1

A total of 135 outbuildings were assigned EF ratings in the El Reno tornado damage path. There were 85 outbuildings rated EF0, 41 EF1, and 9 rated EF2. Most outbuildings were associated with rural residential properties. Generally, these were small, wood-framed structures with metal clad walls and roofs, utilized as barns to store farm equipment or hay (Fig. 11). Total destruction of these buildings (DoD 12) yielded a maximum EF2 rating. In several instances, destroyed outbuildings were adjacent to residences that sustained less severe damage. This indicated to us that failure wind speeds in the EF scale need to be adjusted between outbuildings and residences.



Figure 11. EF1 damage to a metal-clad, wood-framed outbuilding (DoD 6).

4.2 Residences – DI 2

A total of 147 residences were assigned EF ratings in the El Reno tornado damage path. There were 103 residences rated EF0, 24 EF1, 17 EF2, and only 3 rated EF3 (Fig. 12). Residences were rated EF0 if they lost some of their roof covering (DoD 2). An EF1 rating was given to residences that lost a portion of their roof deck (DoD 4). Residences were rated EF2 if they lost most of their roof (DoD 6). Homes with perimeter walls down but interior walls remaining upright were rated EF3 (DoD 8). One residence had all walls down and a pile of debris remaining on its concrete slab foundation. This damage severity was a candidate for an EF4 rating. However, close examination revealed anchor bolts around the foundation perimeter did not have nuts or washers to secure the wall bottom plates (Fig. 13). Since the walls were not anchored to the foundation, damage to this residence was rated EF3 instead of EF4.



Figure 12. Increasing damage ratings to wood-framed houses: a) EF0, b) EF1, c) EF2, and d) EF3.



Figure 13. All walls on this home had collapsed in the center of the tornado path. Close examination revealed no nuts or washers on the anchor bolts (inset a). Therefore, a rating of EF3 was assigned instead of EF4.

4.3 *Manufactured Homes – DI 3 and 4*

A total of 87 manufactured homes were assigned EF ratings within the tornado damage path. These homes had steel undercarriages. There were 31 single-wide and 56 double-wide homes. The maximum (expected value) damage rating for a destroyed manufactured home is EF2. Overall, there were 45 manufactured homes rated EF0, 21 EF1, and 21 EF2.

Generally, these homes sustained more severe damage than adjacent homes constructed on permanent concrete foundations. This indicated to us that failure wind speeds in the EF scale need to be adjusted between manufactured homes and permanent homes. In one instance, the steel frame of a single-wide home was all that remained except for an SUV that came to rest on top of the frame (Fig. 14).



Figure 14. An SUV that came to rest on the steel frame of a destroyed single-wide mobile home.

4.4 *Institutional Buildings – DI 20*

There were three, one-story institutional buildings at the Canadian Valley Technology Center near the north end of the tornado damage path. The northernmost building sustained only roof damage and was rated EF1. The west (main) building was a one-story, steel-reinforced concrete framed structure with concrete masonry unit (CMU) in-fill walls covered with brick veneer. A portion of the masonry wall collapsed at the southeast corner of the building (DoD 7), resulting in this building being rated EF2 (Fig. 15).

A large rectangular building east of the main building contained the Aviation Technology Department. This building experienced partial roof collapse when overhead doors failed allowing internal pressure to lift and fracture several double-tee roof beams. The double tees fractured at midspan and collapsed into the building (Fig. 16). Perimeter walls remained standing. Damage to this building (DoD 8) was rated EF3.

4.5 *Metal Buildings – DI 21*

There were 34 metal building systems within the tornado damage path. These buildings had light steel-framing and exterior metal wall panels. In the EF scale, the maximum (expected value) damage rating for a destroyed metal building would be EF3. There were 21 buildings rated EF0, 7 EF1, 1 EF2, and 5 EF3.

The tornado destroyed all three metal buildings at the Oklahoma West Livestock Market. These buildings were constructed on concrete slab foundations. Steel columns failed where they were attached with anchor bolts to their foundations. Base plates were either torn from the columns when the welds failed or the anchor bolts were pulled through the base plates when deformed (Fig. 17). Damage to these buildings was rated EF3.



Figure 15. Damage to a concrete framed building at the Canadian Valley Technology Center: a) collapse of concrete masonry walls, b) closer view showing the absence of vertical steel reinforcement in the wall. Damage to this building was rated EF2.



Figure 16. Damage to the Aviation Technology Department at the Canadian Valley Technology Center: a) an airplane in the doorway and b) collapsed large span, steel-reinforced concrete double tee roof beams. The beams fractured at midspan due to wind uplift forces. Damage to this building was rated EF3.



Figure 17. Destruction of a metal building at the Oklahoma West Livestock Market. Steel column base plates were: a) torn along welded connections, or b) pulled through their anchor bolts. Damage to this building was rated EF3.

4.6 Electrical Transmission Lines – DI 24

There were numerous wooden power poles damaged by the tornado. Such poles had stood alongside rural roads. The poles were tilted or broken (Fig. 18). A series of 15 double-wood poles were broken along Interstate 40. Tall, galvanized steel, single-pole towers were bent to the east along the west side of Radio Road where residences sustained EFO damage.

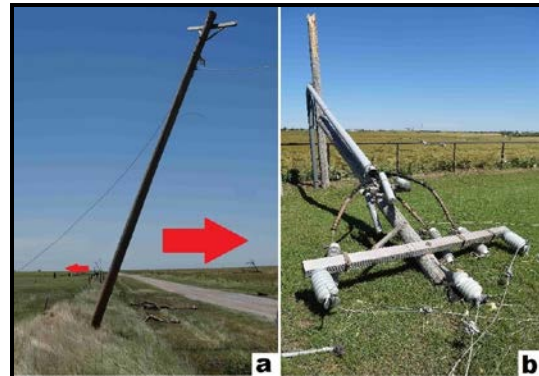


Figure 18. Wind damage to wood power poles: a) leaning poles in opposite directions, and b) a broken pole.

4.7 Trees – DIs 27 and 28

The tornado traversed mostly open country with few trees. Those trees present in the damage path were concentrated around houses and along creeks. Some of the most intense tree damage occurred along Choctaw Road where trees were defoliated, debarked, and had large branches removed (Fig. 19). Such tree damage was rated EF3, the maximum in the EF scale. Many trees had been uprooted in softer soil along creeks and were rated EF1 or EF2.



Figure 19. EF3 damage to trees along Choctaw Road (DoD 5).

5. NON-STANDARD DIs

Survey teams documented 344 non-standard DIs including oil tank batteries, vehicles, parking stops, wheat crops, and road surfaces. These non-standard DIs were not part of the EF-scale rating system, but their conditions were documented as they might be added at a later date. In addition, non-standard DIs are valuable as indicators of the relative strength of a tornado.

5.1 Oil Tank Batteries

There were a total of 112 oil tank batteries within the tornado damage path. These sites contained one or more barrel-shaped steel tanks, a gas separator, and occasionally, a heater treater. The gas separator is a steel tank in which gravity and high pressure spinning motions separate oil from water and gases. Gas separator tanks sat unanchored on a concrete pads. However, gas separator tanks were stabilized laterally by steel piping. Heater treater tanks typically were taller than gas separator tanks and contained heating units to assist in the breakdown of oil, gas, and water. Heater treater tanks also sat unanchored on concrete pads, being stabilized laterally only by piping.

Our survey of oil tank batteries revealed toppled gas separator or heater treater tanks in 30 of the 112 sites. Barrel tanks fell over or were removed from 12 of the 112 locations (Fig. 20). Not surprisingly, the greatest damage to oil tank batteries occurred near the tornado center and to the south where the strongest winds occurred.

We compared the extent of damage to oil tank batteries with nearby DIs and determined that toppling of the gas separator and/or heater treater tanks was consistent with EF1 damage. Toppling of the barrel-shaped steel tank occurred in regions of

EF2 damage, and removal of tanks from a site occurred in regions of EF3 damage. Of course, a primary factor in whether the tanks moved was their weight and how full they were. Team members did not have that information. Still, oil tank equipment was a valuable damage indicator that should be studied further for possible inclusion in the EF scale.



Figure 20. Damage to an oil tank battery near South Country Club Road and 15th Street Southwest.

5.2 Vehicles

Several vehicles were rolled or tossed by the tornado, especially along and east of Highway 81 (Fig. 21). Such vehicle damage typically is associated with violent tornadoes. However, as noted with past studies by Marshall et al. (2008) and Marshall (2010), many factors determine whether vehicles are moved or transported by tornadic winds. Some factors include size, weight, and profile of the vehicle as well as horizontal and vertical components of the wind and acceleration effects. Because of these variables, vehicles are not currently a DI. As noted earlier, all eight fatalities in the El Reno tornado occurred in vehicles (NWS, 2013).



Figure 21. A vehicle flipped onto a pickup truck at the Canadian Valley Technology Center. The building adjacent to these vehicles was rated EF3 damage.

5.3 *Parking Stops*

Several concrete stops had shifted westward in the parking lot at the Canadian Valley Technology Center. These parking stops were between two buildings rated EF1 and EF2, respectively (Fig. 22). The parking stops were secured to the pavement with pairs of steel rebar. The rebar had bent westward when the parking stops moved. Each concrete stop weighed approximately 111 kg. Movement of the parking stops indicated that high wind speeds extended to the ground. Similar observations have been made by Marshall (2012a, 2014) with lofted parking stops in the Joplin, Missouri tornado and shifted parking stops in the Vilonia, Arkansas tornado, respectively.



Figure 22. Westward movement of parking stops at the Vo-Tech Center. Such movement occurred in between buildings rated EF1 and EF2.

5.4 *Wheat Crops*

There were isolated areas and swaths in the tornado path where wheat crops were flattened (Fig. 23). Such evidence indicated that high speed winds reached the ground. However, there was uncertainty in determining the wind speeds necessary to cause such damage, especially since there were no DIs nearby. No ground scouring was found anywhere in the damage path.



Figure 23. A wind-damaged wheat field along Reuter Road where the tornado was most intense.

5.5 *Road gravel*

Intense tornadoes have been known to scour road surfacing as noted by Marshall et al. (2012b) in their survey of the violent Oklahoma tornadoes that occurred on May 24, 2011. Such was the case in the El Reno tornado along Reuter Road where we found two areas of substantial gravel loss (Fig. 24).

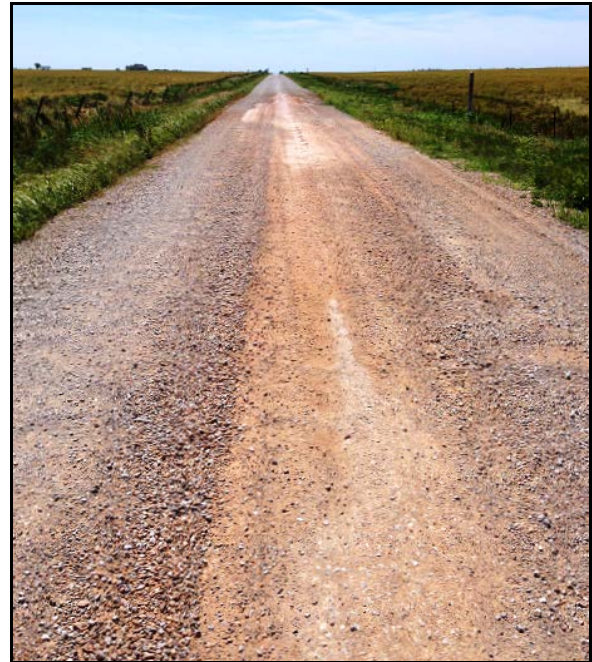


Figure 24. Scouring of the gravel road surface along Reuter Road was evidence strong winds reached the ground. This was near where three storm researchers were killed.

5.6 *Wind Turbine Blade*

There was an unusual non-standard DI found in the El Reno tornado damage path. A 60 m long wind turbine blade was on display at the Canadian Valley Technology Center (Fig. 25). The blade sat in a concrete cradle east of a school building. The blade was lifted from its cradle and transported westward where it came to rest on a school building roof. Damage to the school building, outside the region of the blade impact, was rated EF0.



Figure 25. 60m long wind turbine blade that was on display was lifted from its mooring and deposited on a school building to the west. The inset a) image shows the location of the turbine blade before the tornado. Red arrows indicate how the blade pivoted counterclockwise to the west.

5.7 Storm Shelters

Survey team members found three houses with below ground storm shelters where houses sustained EF2 of EF3 damage. Several people sought refuge in the shelters during the tornado and escaped serious injury. Two shelters had swing doors and one had a sliding door. One of the swing doors was an older model with only a swivel plate lock. The other swing door had a lever handle lock and two, spring-loaded, L-shaped locks. Regardless of the type of door, all performed well during the tornado.

6. RADAR OBSERVATIONS

The El Reno tornado was well sampled by University of Oklahoma's RaXPoL radar. The RaXPoL radar is a rapid-scanning, X-band (3-cm wavelength), polarimetric mobile radar. The radar dish is 2.4 m in diameter and mounted on a high-speed pedestal capable of rotating the antenna at 180 degrees per second. It can complete a 10-elevation, step-volume scan in about 20 s, while maintaining a 180 record-per-second data rate. The transmitter has 20-kW of peak-power using a traveling wave tube amplifier, and pulse compression and frequency hopping waveforms can be used. Frequency hopping permits acquisition of many more independent samples than without frequency hopping. This makes it possible for the radar to scan much more rapidly than conventional radars. Standard data products include vertically and horizontally polarized equivalent radar reflectivity factor, Doppler velocity mean and standard deviation, copolar cross-correlation coefficient, and differential phase. Further characteristics of the RaXPoL radar are presented by Pazmany et al. (2013). Snyder and

Bluestein (2014) and Bluestein et al. (2014a) have shown that the RaXPoL radar has been deployed successfully on a number of tornadic storms.

The RaXPoL radar was located initially just southwest of El Reno and scanned the tornado between 2245 and 2315 UTC at zero degree elevation. Radial velocity bins originally were folded at 30 m s^{-1} intervals, thus it took considerable time and effort to unfold these data. The radar was approximately 9 km east of the tornado when the tornado began, then left the site when the tornado closed to within 6 km south of the radar. The resulting unfolded maximum instantaneous velocities (V_{max}) showed several bins in the 70 to 80 m s^{-1} range with some 90 plus m s^{-1} values west of Highway 81 (Fig. 26). While some high bin values could be correct, some of these anomalies could have been introduced from the automated dealiasing routine. Thus, these radar data later were smoothed using a median filter that calculated a mean value for each bin, within three azimuths and five range gates around each bin. Additional details of RaXPoL deployment during the El Reno storm and subsequent analysis can be found in Snyder and Bluestein (2014) and Bluestein et al. (2014 b).

As the tornado crossed Highway 81, the RaXPoL radar moved east to the Interstate 40 and Banner Road location and scanned the tornado from 2324 through 2326 UTC. The tornado became quite intense east of Highway 81 with maximum velocities exceeding 120 m s^{-1} (Fig. 27) within subvortices just northeast of the intersection of Radio and Reuter roads. It was at this location that three storm researchers were killed. The radar truck had to move again when the tornado turned northeast and closed to within 3 km. At that time the leading edge of the RFD gust front was within 0.5 to 1 km of the radar location.

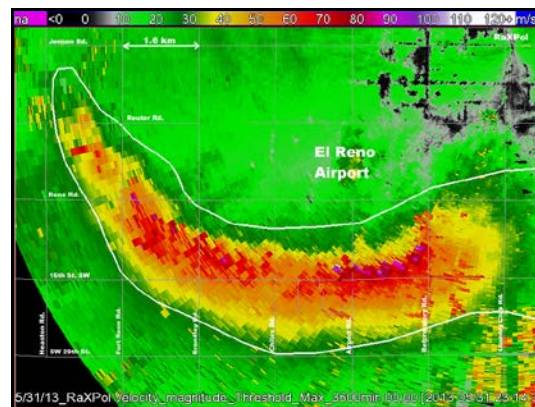


Figure 26. Maximum velocities of the El Reno tornado at zero degree elevation (not smoothed) obtained while the tornado was west of Highway 81. The white outline is the 30 m s^{-1} isodop.

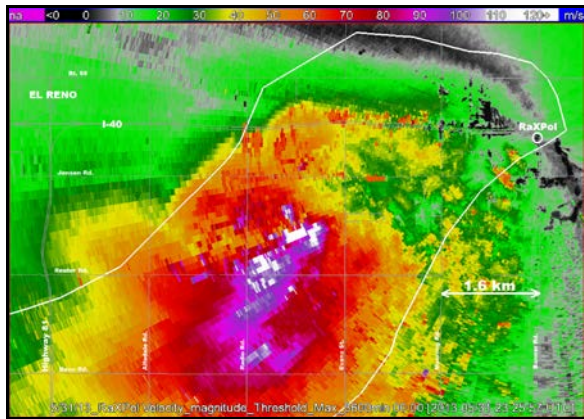


Figure 27. Maximum velocities of the El Reno tornado at zero degree elevation (not smoothed) obtained from 2324 to 2326 UCT while the tornado was east of Highway 81. The radar was located in the upper right corner of the image. The white outline is the edge of the tornado as determined by the 30 m s^{-1} isodop.

Analysis of radar velocities indicated there were vortices of various sizes. The largest circulation was the parent mesocyclone which included a strong RFD. The main tornadic circulation contained a persistent subvortex while intermittent subvortices rotated around the periphery of the main tornado (Fig. 28). Wurman et al. (2014) also observed these subvortices with the DOWs. In addition to the subvortices, there were satellite tornadoes moving southbound into the northwest flank of the main tornado and anticyclonic tornadoes east-southeast of the main tornado. Some of the subvortices, including the anticyclonic tornadoes, had smaller subvortices vortices. The various sizes and types of vortices made it more difficult for surveyors to determine what vortex caused what damage, especially in such a sparsely populated, rural area.

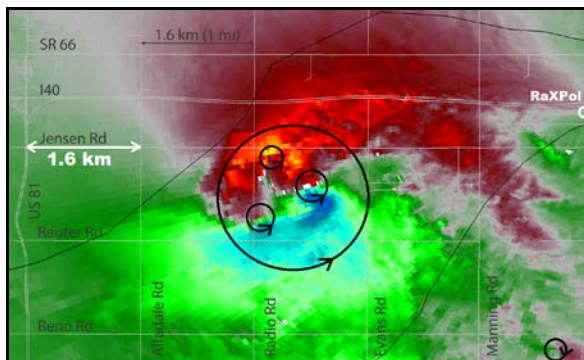


Figure 28. Radial velocity image taken at 2326 UTC showing the large tornadic circulation, and subvortices (circled). The anticyclonic tornado is located in the lower right corner of the image.

6.1 Radial Velocity-Damage Comparison

EF-scale damage ratings were overlaid onto the radar-derived velocities for comparison purposes. Such comparisons between damage and radar velocity measurements have been made by Wurman and Alexander (2005) in their analysis of the Spencer, SD tornado. EF-scale damage ratings are based on expert elicitation estimates of failure wind velocities that have 3 s duration, at 10 m above the ground, in open, unobstructed terrain. By contrast, radial velocities are instantaneous, area-averaged, reflectivity-weighted measurements at various heights and ranges. These differences must be kept in mind when comparing damage with radar velocity measurements.

The El Reno tornado traveled through a subdivision west of Highway 81 causing EF1 to EF3 damage (Fig. 29). The associated EF wind speeds to cause such damage were between 38 and 74 m s^{-1} . By comparison, the RaXPol Vmax was between 50 and 80 m s^{-1} . Thus, RaXPol values were approximately 10-30% higher than EF values for reasons mentioned previously. Wurman and Alexander (2005) made the same observation in their paper.

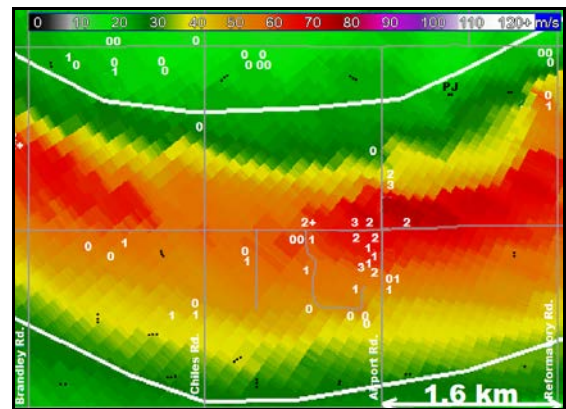


Figure 29. Color-coded map of smoothed Vmax west of Highway 81 where the center of the tornado traveled through a subdivision. EF ratings are overlaid. The white outline is the boundary of the tornado as determined by the 30 m s^{-1} isodop.

The highest velocity measurements from the RaXPol radar occurred east of Highway 81 near Radio and Reuter roads (Fig. 30). This was a sparsely populated area with open fields. Even when smoothed, the velocities exceeded 100 m s^{-1} . Radar measurements indicated this tornado could well have reached EF5 intensity, however, there were no DIs where Vmax was highest. That said, however, there was an absence of ground scouring or substantial damage to nearby oil field equipment in this area.

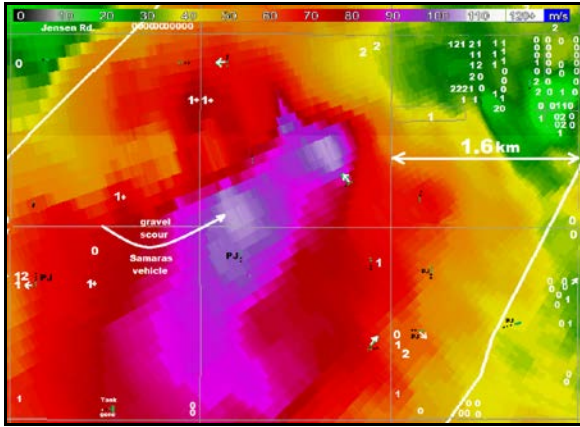


Figure 30. Color-coded map of smoothed Vmax east of Highway 81 where the tornado traveled through open fields where there were no buildings. EF ratings are overlaid. The white outline is the boundary of the tornado as determined by the 30 m s⁻¹ isodop.

7. SUMMARY

The El Reno tornado began as a multi-vortex that moved southeast, then turned east as it crossed Highway 81, then turned northeast before making a loop near Interstate 40 dissipating near Banner Road. The tornado traveled 26.2 km and the maximum damage rating was EF3.

The El Reno tornado presented many challenges to damage surveyors as the tornado traveled mostly through sparsely populated areas, in open terrain, with relatively few trees. Damage survey teams had difficulty determining the characteristics of the tornado such as path length, path width, and what wind features caused the damage. The RaXPol radar provided crucial information that helped clarify the dimensions of the tornado damage path and indicated the highest velocities occurred in areas notably absent of DIs. The 30 m s⁻¹ isodop was utilized to determine the width of the tornado, the maximum being 4.2 km.

Survey teams rated 257 DIs and documented damage to an additional 344 non-standard DIs, which included analysis of 112 oil tank batteries. The most common DIs were single-family houses, outbuildings, and manufactured homes. One house had all walls down and a pile of debris on its foundation. This was the only candidate for an EF4 rating. However, wall plates were not attached to the concrete slab foundation as nuts and washers were missing from the anchor bolts. This deficiency led team members to rate the home EF3 instead of EF4. There were large gaps in the tornado path where there were few or no DIs. Twenty-five of the 39 square mile blocks had fewer than 10 DIs each. By comparison, the Moore, OK tornado (which occurred

11 days earlier) had 4222 DIs or 16 times as many DIs since the Moore tornado traveled through more densely populated areas. Clearly, the more DIs there are in a tornado path, the more likely it is to sample the highest wind speeds.

The RaXPol radar obtained high resolution velocity data at zero degree elevation in close proximity to the tornado. Radar analysis revealed the tornado grew in size and intensity west of Highway 81 where peak velocities were near 90 m s⁻¹. The tornado continued to intensify after it crossed Highway 81, exhibiting subvortices which moved rapidly around the periphery of the main tornado. There also was a more permanent vortex or “tornado within a tornado” feature. These subvortices were associated with peak velocities in excess of 120 m s⁻¹.

Radar and storm chaser observations/videos revealed detailed complexities of the El Reno tornado that could not have been determined by the ground survey alone. The tornado had vortices of various sizes and durations. Damage was caused by strong RFD winds in the mesocyclone, the main tornado, a persistent subvortex, intermittent subvortices, satellite tornadoes, and anticyclonic tornadoes. Thus, accuracy of the damage survey was improved by utilizing radar and storm chaser information and having some of this information available during the survey. Subsequent analysis of aerial imagery by Atkins et al. (2014) revealed details that were not readily visible from the ground. They mapped debris swaths and movement of hay bales and oil tanks. Areas of flattened wheat were quite visible from the air. Their study demonstrated the importance of conducted aerial surveys after tornadoes.

A comparison between EF ratings and maximum velocities determined by the RaXPol radar indicated RaXPol values were 10 to 30 percent higher than EF values. This difference can be explained by how EF ratings and radial velocities are determined. Even if RaXPol velocities were reduced 25 percent to match EF-scale wind speeds, the maximum radar-derived velocities would be in the EF5 range near Radio and Reuter roads. However, there were no DIs in the region where RaXPol velocities were maximum.

A perplexing issue was the absence of ground scouring of wheat fields where Vmax was highest. Also, nearby oil tank battery damage was less severe damage than where the tornado was weaker, west of Highway 81. Perhaps short residence times of high velocity winds over a point (bursts less than one second) causes less damage as suggested by Wurman et al. (2014), and results in lower damage ratings. By contrast, Phan and Simiu (1998) have argued that wind velocities of longer duration caused more intense damage and therefore, damage ratings were overestimated in the Jarrell, Texas tornado.

8. ACKNOWLEDGEMENTS

The authors would like to thank Nolan Atkins, C. S. Kirkpatrick, James G. LaDue, Kay Marshall, and Greg Stumpf who reviewed the paper.

Funding for the radar analyses were supported in part by NSF grants AGS- 0934307, AGS-1262048, AGS-0821231, and AGS-1237404. John Meier at the Advanced Radar Research Center at the University of Oklahoma (OU) maintained RaXPol for use during the 2013 field experiment and OU provided matching funds for the MRI grant that funded the construction of the radar. Funding for CIMMS authors was provided by NOAA/Office of Oceanic and Atmospheric Research under NOAA-University of Oklahoma Cooperative Agreement NA110AR430072, U.S. Department of Commerce.

9. REFERENCES

Adams, R., 2005: An examination of the 22 May 2004 Hallam, Nebraska tornado, 4th Amer. Meteor. Soc. Student Conference, 85th Annual meeting, San Diego, CA. Poster session. Available online at: <https://ams.confex.com/ams/Annual2005/webprogram/Paper88523.html>

Atkins, N., R. Wakimoto, K. Butler, H. Bluestein, K. Theim, J. Snyder, J. Houser, and J. Wurman, 2014: Aerial damage survey and high resolution dual-polarization radar analysis of the 2013 El Reno tornado, 27th Conf. on Severe Local Storms, Madison, WI. Available online at: <https://ams.confex.com/ams/27SLS/webprogram/Paper254162.html>

Bluestein, H. B., J. C. Snyder, K. J. Thiem, Z. B. Wienhoff, J. B. Houser, and V. Mahale, 2014a: Recent observations of tornadoes using a mobile, rapid-scan, polarimetric, X-band, Doppler radar. Eighth European Conference of Radar Meteorology and Hydrology, 4 Sept. 2014, Garmisch - Partenkirchen, Germany, 10 pp. Available online at: http://www.pa.op.dlr.de/erad2014/programme/ExtendedAbstracts/012_Bluestein.pdf

_____, _____, and J. B. Houser, 2014b: A multi-scale overview of the El Reno, Oklahoma tornadic supercell of 31 May 2013. *Wea. Forecasting* (in review)

Marshall, T. P., D. McCarthy, and J. Ladue, 2008: Damage survey of the Greensburg, KS tornado, 24th Conference on Severe Local Storms, Savannah, GA. Available online at:

<http://ams.confex.com/ams/pdfpapers/141534.pdf>

_____, 2010: Damage survey of the Picher, Oklahoma tornado, 25th Conference on Severe Local Storms, Denver, CO. Available online at: <http://ams.confex.com/ams/pdfpapers/173923.pdf>

_____, W. Davis, and S. Runnels, 2012a: Damage survey of the Joplin Tornado: 22 May 2011, 26th Conf. Severe Local Storms, Nashville, TN, 21 pp. Available online at: <https://ams.confex.com/ams/26SLS/webprogram/Paper211662.html>

_____, J. G. Ladue, K. L. Ortega, and G. J. Stumpf, 2012b: Performance of residences and shelters in the Oklahoma tornadoes of 24 May 2011, 26th Conf. Severe Local Storms, Nashville, TN, 12 pp. Available online at: <https://ams.confex.com/ams/26SLS/webprogram/Paper211671.html>

_____, J. Robinson, E. Kiesling, and L. Tanner, 2014: Damage survey of the Mayflower-Vilonia, Arkansas tornado. 27th Conf. on Severe Local Storms, American Meteorological Society, Madison, WI. Available online at: <https://ams.confex.com/ams/27SLS/webprogram/Manuscript/Paper254346/MayflowerV3.pdf>

National Weather Service, 2013: STORM DATA, May issue, p.467. Available online at: <http://www1.ncdc.noaa.gov/pub/orders/IPS/IPS-E1F99F07-9A40-483A-9BFA-F2069AEF41C0.pdf>

Pazmany, A. L., J. B. Mead, H. B. Bluestein, J. C. Snyder, and J. B. Houser, 2013: A mobile, rapid-scanning, X-band, polarimetric (RaXPol) Doppler radar system. *J. Atmos. Ocean. Technol.*, **30**, 1398 – 1413. Available online at: <http://journals.ametsoc.org/doi/abs/10.1175/JTECH-D-12-00166.1>

Phan, L.T. and E. Simiu, 1998: The Fujita Tornado Intensity Scale: A critique based on observations of the Jarrell, Texas tornado of May 27, 1997, Building and Fire Research Laboratory, National Institutes of Standards and Technology Technical Note 1426, 23 pp. Available online at: http://www.nist.gov/customcf/get_pdf.cfm?pub_id=908754

Snyder, J. C., and H. B. Bluestein, 2014: Some considerations for the use of mobile Doppler radar data for tornado intensity determination. *Wea. Forecasting*, **29**, 799-827.

Wakimoto, R. N. Atkins, K. Butler, H. Bluestein, K. Thiem, J. Snyder, J. Houser, 2014: The El Reno Tornado: Mobile polarimetric radar data and photogrammetric analysis. Presented at the 27th Conf. on Severe Local Storms, Madison, WI. Available online at:
<https://ams.confex.com/ams/27SLS/webprogram/Paper254288.html>

Wind Science and Engineering Center, 2006: A recommendation for an enhanced Fujita scale, 111 pp. Available online at:
<http://www.depts.ttu.edu/weweb/efscale.pdf>

Wurman, J., C. Alexander, 2005: The 30 May 1998 Spencer, South Dakota, Storm. Part II: Comparison of Observed Damage and Radar-Derived Winds in the Tornadoes, *Mon. Wea. Rev.*, **133**, 97-119. Available online at:
<http://journals.ametsoc.org/doi/pdf/10.1175/MWR-2856.1>

Wurman, J., K. Kosiba, P. Robinson, and T. Marshall, 2014: The role of multiple-vortex tornado structure in causing storm researcher fatalities. *Bull. Amer. Meteor. Soc.*, **95**, 31-45. Available online at:
<http://journals.ametsoc.org/doi/abs/10.1175/BAMS-D-13-00221.1>